



An efficient photocatalytic degradation of Quinalphos pesticide under visible light using zinc oxide/magnesium oxide nanocomposites as a novel photocatalyst

S Sibmah* & E K Kirupavasam

Department of Chemistry & Research Centre, Nesamony Memorial Christian College, Marthandam 629 165, Tamil Nadu, India

E-mail: sibmah1998@gmail.com

Received 20 January 2022; accepted (revised) 13 April 2022

About one million tons of pesticide effluents were discharged into natural streams and water bodies from local industries and agricultural fields. In view of growing environmental issues there is a requirement for the termination of pesticides and its residues from local and commercial water streams. Photocatalytic degradation method is regarded as a convenient method for the treatment of organic contaminants because of its low cost, lack of secondary pollutants and eco-friendly character. In this study, an enhanced and visible light effective ZnO/MgO nanocomposite photocatalyst has been synthesized by a wet chemical method using zinc acetate dihydrate and magnesium chloride as precursor. The prepared sample has been examined to diagnose its structural, morphological, optical and fluorescence properties using XRD, UV-Vis, SEM, EDX, FT-IR and fluorescence spectral analysis. The organophosphorus pesticide, Quinalphos, has a wide application worldwide, particularly to control the population of pests. Due to its toxic character, it is necessary to eradicate Quinalphos and its residues from the environment. The synthesised ZnO/MgO nanocomposite is analysed to degrade Quinalphos pesticide under direct sunlight at neutral pH. The photocatalytic performance of ZnO/MgO nanocomposite is examined by loading 4 mg/L of the catalyst in 20 ppm of the Quinalphos solution to achieve 98% degradation within forty minutes. Moreover, this nanocomposite could be separated and utilised up to five cycles with no change in its activity.

Keywords: Pesticide, nanocomposite, contaminants, Quinalphos, photocatalysis, visible light

Wastewater discharged from various industries constitute of multiple contaminants such as heavy metals, pesticide, dyes, antibiotics, etc¹. Nowadays pesticides are broadly utilised for the protection of food crops and to upgrade crop productivity. Moreover, these pesticides also have an extensive application in various industries such as carpet industry, paper industry, leather industry, etc. However, at the same time the pesticides have created an extreme damage to human health and the environment. The uncontrolled usage of pesticides and organic chemicals for paper, leather, paint and wood conservation units have given rise to an acute contamination of water². The organophosphorus pesticides are widely used all around the world³. Quinalphos is an organophosphorus pesticide applied widely for the protection and high productivity of crops like vegetables, tea, cotton and fruits. Extensive usage of Quinalphos likely reaches the aquatic environment and damage the health of aquatic creatures. Moreover, its sediments present in the soil percolate into the water streams and eventually reach the ocean triggering environmental damage.

In recent years, a great deal of attraction has been received by photocatalysis for intensifying the deterioration of organic pollutants including pesticides, industrial chemicals and textile dyes. Photocatalysis is a chemical operation in which a set of chemical reaction is propelled in the presence of light⁴. In this process, semiconductor materials could generate charge carriers in the presence of light radiation, that bring about a sequence of chemical reaction like organic contaminant degradation, redox modification of heavy metals and reduction of carbon monoxide⁵. Photocatalysis is an advanced oxidation process which extremely relies upon hydroxyl radicals that stimulate the elimination of organic compounds that exist in water⁶. The photocatalytic reaction is initiated just when a photocatalyst afflicted with a photon that posse's highest energy in contrast to its bandgap. An electron hole pair was emerging at the time in which the electrons present in the valence band get excited to the conduction band. The electron present in the conduction band of the photocatalyst is later hunted by the oxygen molecules to organise superoxide ions. A persistent attack by the

hydroxyl radicals together with superoxide ions finally brings about the degradation of organic contaminants⁷. Photocatalytic degradation technique is more significant when compared to other degradation techniques since it is more efficient, sludge free and the eradication of organic contaminants present in water could be eliminated by an eco-friendly procedure⁸.

Semiconductor nanomaterials are extensively studied for the degradation of organic contaminants from aqueous phase⁹. ZnO is a semiconductor which has received a great attention due to its abundance, eco-friendly and nontoxic nature. These properties had made this material captivating for various applications like solar cell, optical coatings, photocatalysts, sensors and electrical devices¹⁰. Researchers have exhibited that, for the elimination of organic contaminants in water, ZnO exhibits more desirable photocatalytic activity than TiO₂¹¹. In view of the existence of surface oxygen vacancies and increase in surface area, the photocatalytic activity of doped ZnO is better than undoped ZnO. However, two drawbacks have suppressed the application of ZnO nanoparticle i.e., photo corrosion and its solubility at high pH¹². In order to enhance the activity and stability of ZnO, the prepared ZnO nanoparticle is doped with other metal oxide. Most of the literatures have reported that doping increases the surface area of the metal oxide and this emphasizes the photocatalytic capacity of the metal oxide¹³. Among the numerous metal oxides, MgO exhibits better photocatalytic activity due to its wide band gap¹⁴, low dielectric constant and refractive index. ZnO/MgO nanocomposite is utilised as an effective photocatalyst for the degradation of toxic and harmful organic contaminants in water. Yet, only a very few studies are available on the photocatalytic degradation of Quinalphos using metal oxide nanoparticles. However, in the majority of the reported work, the photodegradation of Quinalphos consumes more time with low degradation efficiency^{15, 16}. Renuka et al. (2022) has studied, 84% degradation of Quinalphos using GO doped ZnO within 45 minutes under UV light¹⁵. Nidhi et al. (2019) has reported 87.5% of Quinalphos degradation within 240 minutes using Mn-N-codoped TiO₂ under visible light¹⁷. The objective of this work is to develop an efficient and economic photocatalytic nanocomposite and to suggest a commercial and effective degradation method to

neutralize Quinalphos present in water within a short span of time under sunlight.

Materials and Methods

All the chemicals were of analytical grade. The chemicals were utilised as received without further purification. Zinc acetate dihydrate [Zn (CH₃CO₂)₂.2H₂O] and Magnesium chloride (MgCl₂) were purchased from Iso-Chem laboratories Kochi (India) respectively. Ammonium hydroxide (NH₄OH) was purchased from Merck specialities pvt. Ltd. Mumbai (India) and doubly distilled water is used throughout the experiment.

Synthesis of ZnO/MgO nanocomposite

Zinc oxide nanoparticles were prepared by dissolving required amount of Zinc acetate dihydrate [Zn (CH₃CO₂)₂.2H₂O] in 100 ml of double distilled water. To the dissolved suspension calculated amount of Ammonium hydroxide (NH₄OH) solution is added drop wise and the solution is stirred for 4 hrs. The supernatant solution was discarded and centrifuged. The obtained precipitate was dried on a hot plate at 80°C and was crushed using an agate mortar pestle to form a fine powder of ZnO.

ZnO/MgO nanocomposite was prepared by mixing a small amount of synthesised ZnO with calculated quantities of Magnesium chloride (MgCl₂). Ammonium hydroxide (NH₄OH) solution was added drop wise and stirred for one hour. The supernatant solution was discarded and centrifuged. The precipitate was dried on a hot plate at 80°C and crushed in an agate mortar pestle to obtain ZnO/MgO nanocomposite¹⁸.

Experimental Section

The experiment was executed at neutral pH by the addition of 4 mg of ZnO/MgO nanocomposite to 20 ppm of the aqueous Quinalphos solution. Before the solution was irradiated under direct sunlight the test solution was stirred under the dark condition for 30 minutes to obtain adsorption - desorption equilibrium. Then the stirred test solution was placed under direct sunlight¹⁹. For each 10 minutes about 3 ml of the test solution was drawn out, followed by centrifugation to remove the catalyst particles from suspension in order to analyse the concentration of Quinalphos after irradiating under direct sunlight. The percentage of degradation was calculated with the aid of the formula given;

$$\% \text{ Of degradation} = \frac{C_0 - C}{C_0} \times 100$$

where, C_0 is the initial concentration of the test solution and C is the concentration of the solution after photocatalytic degradation²⁰.

Photocatalytic degradation studies

Figure 1 exhibits a photograph displaying a change in colour of the solution under study. The out comings obtained in this investigation was fascinated in terms of recognising ZnO/MgO nanocomposite for

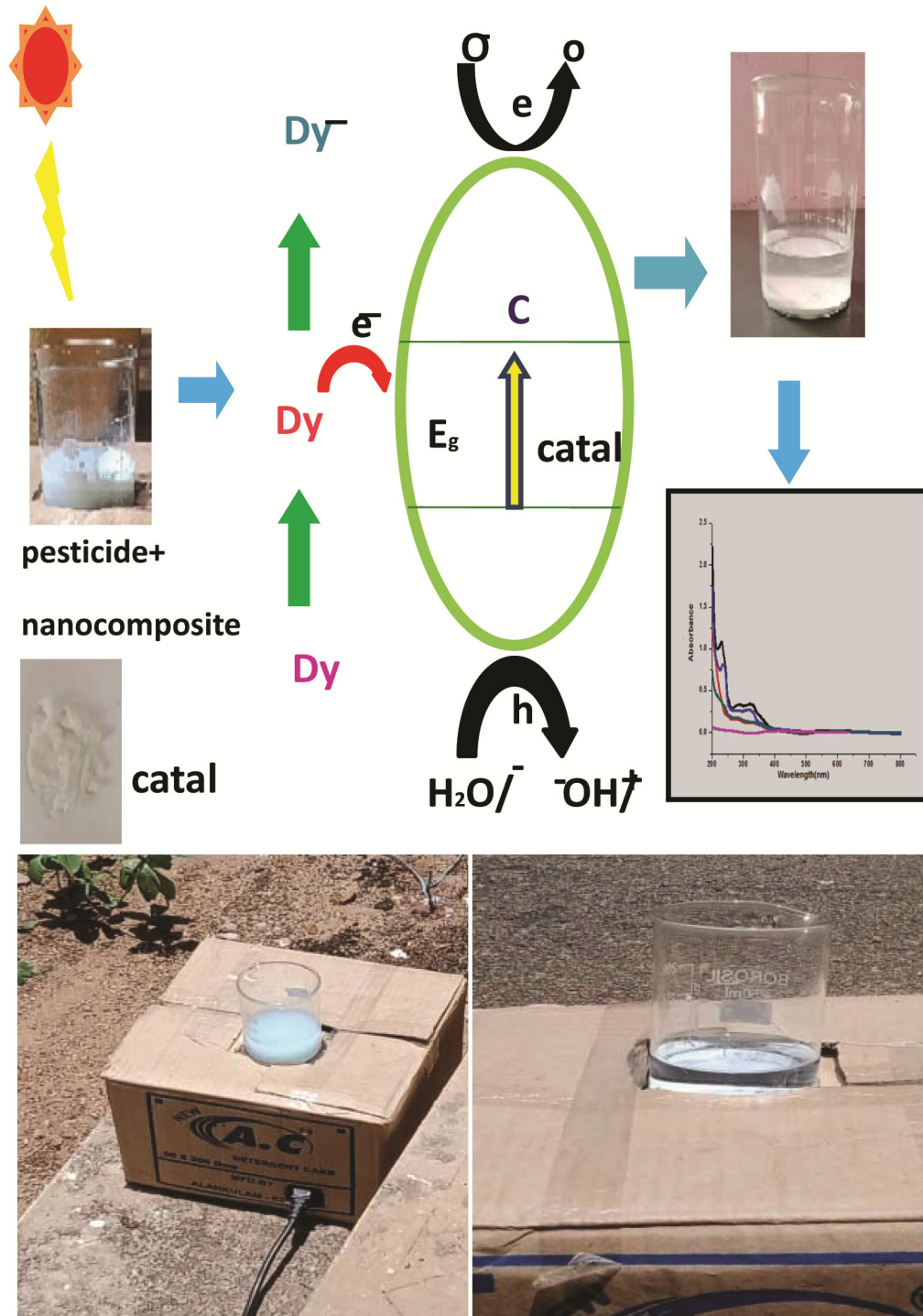


Figure 1 — Visual representation of photocatalytic degradation experiment

degrading Quinalphos in direct sunlight. It was noticed that the colour of the test solution has been changed from pale blue to a colourless clear solution within forty minutes of irradiation showing 98% of degradation in the presence of visible light.

Absorption spectral analysis

The photocatalytic degradation reaction was performed under direct sunlight radiation, using ZnO/MgO nanocomposite as a photocatalyst. The absorption spectra are detected at regular intervals to analyse the degradation of Quinalphos. From this measurement the affinity between the pesticide molecule and the nanocomposite material has been determined and this has made the photodegradation process more efficient. The results are shown in Figure 2. The maximum absorption peak for the pesticide contaminant at 240 nm^{21} has been diminished at an incredible rate and almost disappeared for forty minutes light illumination in the presence of ZnO/MgO nanocomposite.

Characterisation

The size and crystalline phase of the sample was recognised using a Bruker D8 advance X-ray diffractometer (XRD) with Cu K α radiation 40 mA with a scanning rate of 2° min^{-1} . The optical properties of the sample were deduced by Li-2900 UV-Visible spectrometer. The surface morphology and shape analysis were done using Scanning Electron Microscope (model Jeol's 5800LV). Elemental composition was analysed by using Energy

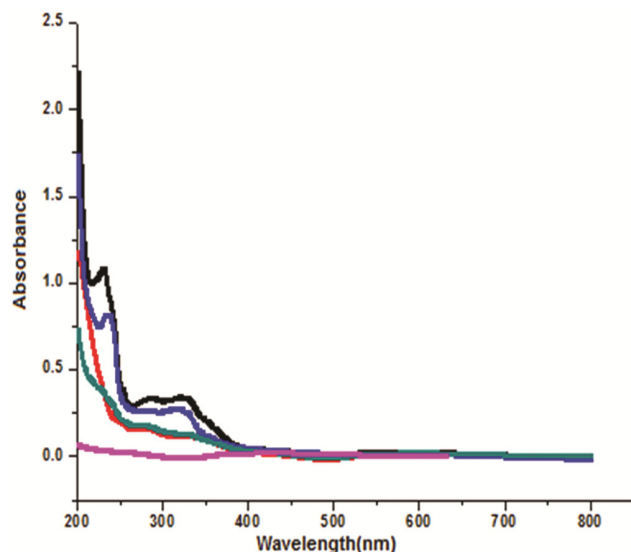


Figure 2 — UV-Visible absorption spectrum for degradation at various intervals of time

Dispersive X-ray spectrometry (EDS) analysis (model JSM-7100F). The surface chemical structure of the nanocomposite sample was studied by using a Bruker Invenio FT-IR spectrometer. The fluorescence property of this nanocomposite was examined by using Spectrofluorimeter (model RF-5301).

Results and Discussion

X-ray diffraction (XRD) analysis

The X-ray diffraction is a non-destructive technique suited to examine the crystalline structure of materials. Figure 3 shows a standard XRD pattern of the ZnO/MgO nanocomposite. The diffraction peaks located at 31.93° , 34.54° , 36.33° , 47.68° , 56.82° , 68.17° , 69.16° (JCPDS card no: 36-1451) correspondingly designated the presence of hexagonal phase of zinc oxide²². The diffraction peaks at 36.41° , 42.96° , 56.82° , 63.01° (JCPDS card no: 45-09646) specify the existence of cubic phase of magnesium oxide²³. The good crystalline nature of the synthesized product is stipulated from the sharp diffraction peaks. Eventually, an average crystal size of the ZnO/MgO nanocomposite was executed for each peak emerged on the XRD diffraction. The size of the nanocomposite was evaluated by using Debye-Scherrer equation. The average size of the synthesized nanocomposite was 32 nm. This was evaluated from the most intense peak obtained from the XRD pattern of the prepared ZnO/MgO nanocomposite.

UV-Visible spectroscopy

The light absorbing capacity of ZnO/MgO nanocomposite was ascertained by the UV-Visible

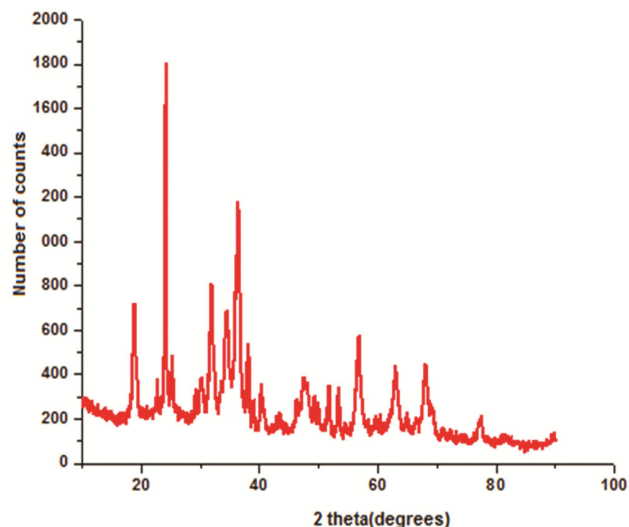


Figure 3 — XRD pattern of ZnO/MgO nanocomposite

spectrum as shown in the Figure 4. The synthesised ZnO/MgO nanocomposite has exhibited a strong absorption at the wavelength of 425 nm. The outcomings from the UV-Visible spectrum designated that the prepared nanocomposite has the potential to absorb visible light²⁴. The stronger absorbance intensity and the larger absorbance region indicated

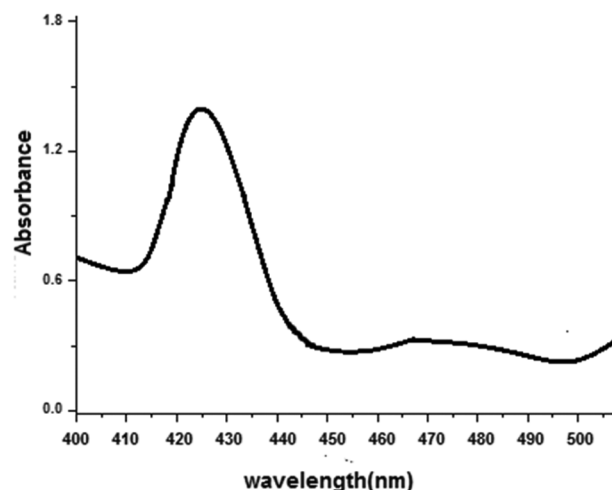


Figure 4 — UV-Visible spectrum of ZnO/MgO nanocomposite

enhanced photocatalytic behaviour of the prepared nanocomposite under direct sunlight.

SEM Analysis

The surface morphology of the synthesized ZnO/MgO nanocomposite was evaluated through SEM analysis. It was noticed that, nearly most of the grains lie within the nanoscale region. The aggregation of the particles on the surface of the catalyst is also observed. However, the sample revealed a regular flake like morphology as it can be seen from the SEM image. The morphology of the prepared sample expressed an efficient photocatalytic activity for the degradation of organic compounds (Quinalphos). This enhanced activity is acquired due to its larger specific surface area and excellent crystallinity of the synthesized ZnO/MgO nanocomposite²⁵. The SEM image of the prepared nanocomposite is shown in Figure 5.

EDX Analysis

In order to authorise the purity of the prepared ZnO/MgO sample, EDX interpretation was analysed as shown in Figure 6. The attributing peaks representing zinc, magnesium and oxygen were

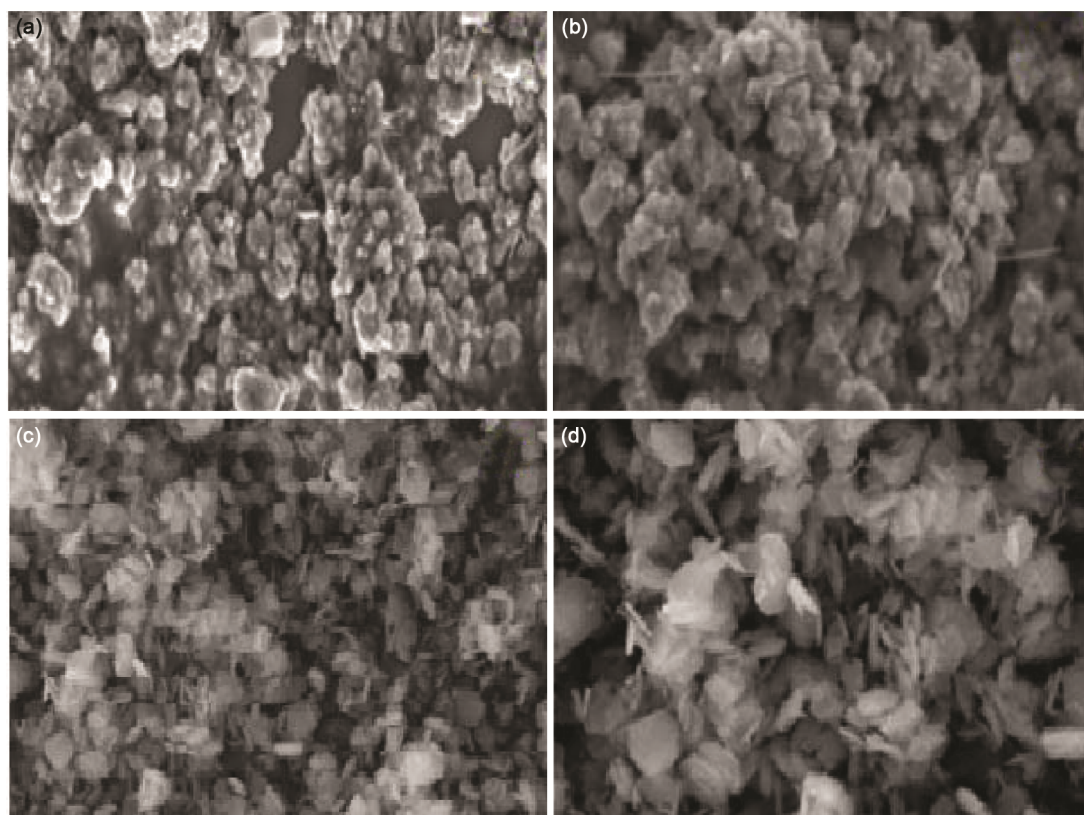
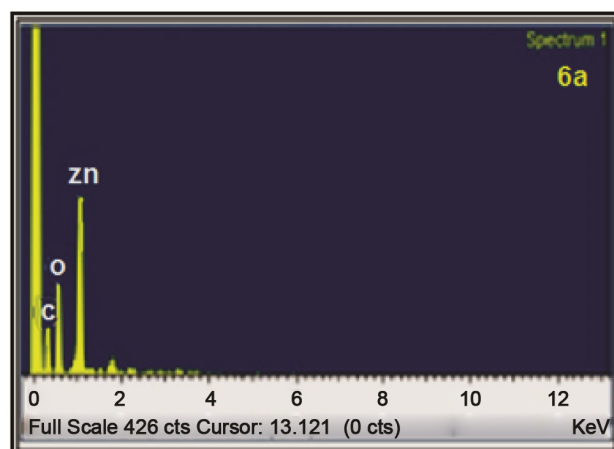
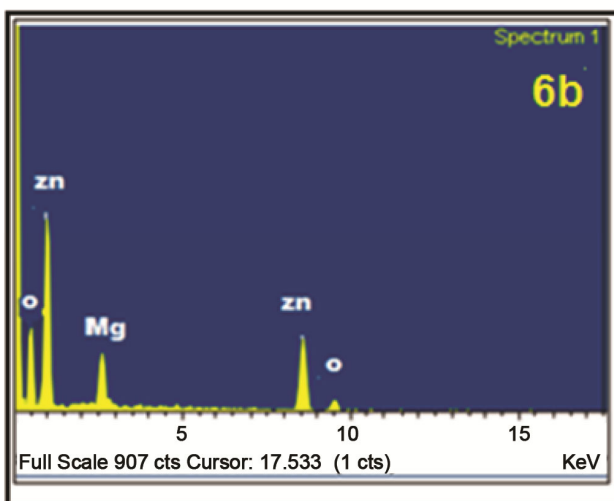


Figure 5 — (a, b) SEM image of ZnO nanoparticle and (c, d) SEM image of ZnO/MgO nanocomposite



Elements	Weight percentage	Atomic percentage
Zinc	51.30	21.71
Oxygen	41.40	71.13
Carbon	7.30	7.16



Elements	Weight percentage	Atomic percentage
Zinc	42.05	35.25
Magnesium	33.54	40.50
Oxygen	24.41	24.25

Figure 6 — (a) EDX pattern of ZnO nanoparticle and (b) EDX pattern of ZnO/MgO nanocomposite

found, but there are no additional peaks which further certify about the purity of the synthesized ZnO/MgO nanocomposite. The weight percentage of magnesium, zinc and oxygen is 33.54%, 42.05%, 24.41% respectively. This designated that the prepared nanocomposite was composed of zinc, magnesium and oxygen without any other foreign elements.

FT-IR analysis

Fourier Transform Infrared Spectroscopy was used to explore the structure, nature and purity of the

prepared nanocomposite²⁶. The broadband at 500-600 cm^{-1} is due to the metal oxide stretching, which corresponds to the formation of metal oxide. The peak at 582 and 833 cm^{-1} is due to the presence of ZnO/MgO bonds, which assure the formation of pure and composite form of the prepared nanocomposite¹⁸. The peaks appeared at 1511 and 1417 cm^{-1} corresponds to the presence of a metal carbonyl and C-H bending²⁷. The peaks at 2883 cm^{-1} denoted the presence of the residual organic component. The FT-IR analysis showed a broad spectrum at 3437 and 3446 cm^{-1} due to -OH stretching vibration in ZnO/MgO nanocomposite²⁸. The FT-IR interpretation was analysed from Figure 7.

Fluorescence studies

The fluorescence spectrum of ZnO/MgO nanocomposite is shown in Figure 8. The broad and strong emission peaks at a range of 400 to 445 nm represented the existence of zinc interstitial defects and is responsible for the cubic shape of magnesium oxide nanocrystals which is in good agreement with the XRD spectrum. Moreover, broader spectrum is responsible for the fluorescence character of the prepared nanocomposite. The peak that appeared at 553 nm indicated the presence of oxygen, zinc and magnesium vacancies. These intrinsic defects are allocated for the recombination of photogenerated holes with the electrons²⁹ and are also responsible for the enhanced photocatalytic performance³¹ of ZnO/MgO nanocomposite.

COD Analysis

The organic strength of industrial effluents is generally estimated by the COD analysis. From this analysis the complete proportion of oxygen necessary for the oxidation of organic materials to carbon dioxide and water can be estimated. The COD of the pesticide solution before and after degradation was determined. The initial and final COD value for the pesticide contaminant was found to be 11614 mg/L and 162 mg/L respectively. The reduction in COD measurements certified the decomposition of pesticide molecules together with the removal of colour³⁰.

Total Organic Carbon (TOC) Analysis

The total amount of organic carbon for this degradation study is estimated by TOC. It is widely used to quantify the organic carbon content present in industrial effluent streams. It is considered more significant, because it can be applied for the evaluation of advanced oxidation process such as

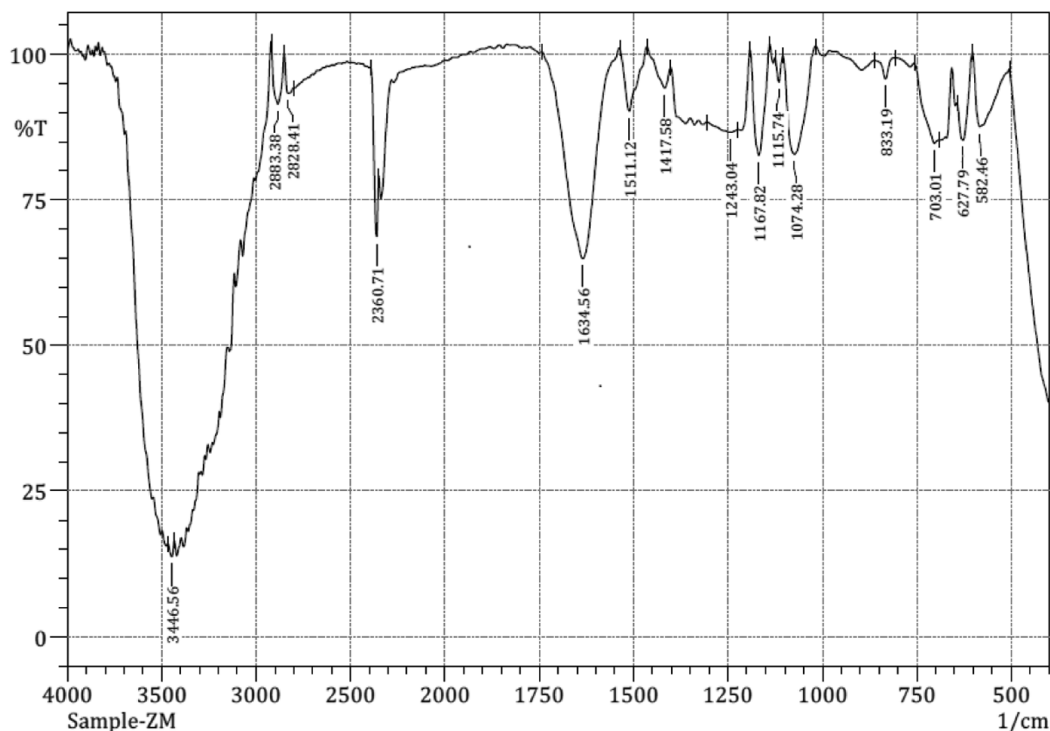


Figure 7 — FT-IR spectra for ZnO/MgO nanocomposite

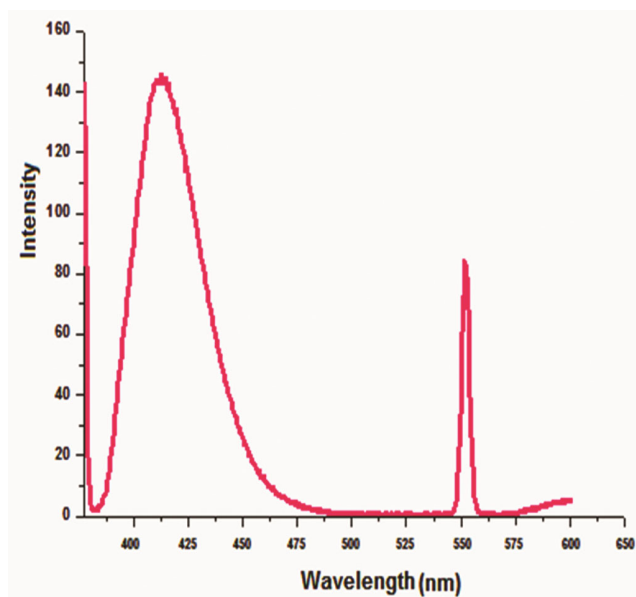


Figure 8 — Fluorescence spectra for ZnO/MgO nanocomposite

photocatalysis³¹ which has been formulated to degrade a wide range of organic and inorganic contaminants. About 90% of organic carbon terminated from the Quinalphos solution within forty minutes which has been achieved by using ZnO/MgO nanocomposite through photodegradation. From this evaluation, it is

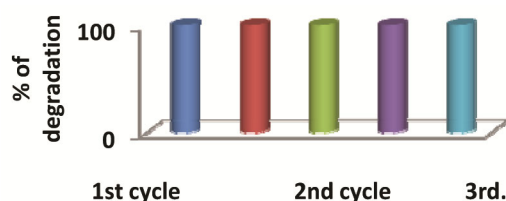


Figure 9 — Recycling ability of ZnO/MgO nanocomposite

observed that ZnO/MgO nanocomposite is an efficient photocatalyst to degrade pesticide pollutants.

Recycling ability of the catalyst

The recycling ability of the photocatalyst significantly raises the application cost and stability of the catalyst³². Figure 9 represented the recycling ability of the catalyst. To check out the recycling ability of the prepared nanocomposite, the designated nanocomposite was collected by centrifugation from the test solution after completion of degradation. The retrieved nanocomposite was washed in double distilled water, filtered, dried and utilised for the next degradation cycle of Quinalphos. This procedure was repeated for more cycles and the degradation efficiency of Quinalphos remains the same for five cycles which is substantiated from UV-Visible absorbance data. This has obviously specified the

auspicious recycling capacity of the prepared ZnO/MgO nanocomposite.

Conclusion

The visible light active ZnO/MgO nanocomposite was synthesized by wet chemical method. Further, the prepared nanocomposite was examined by FT-IR, XRD, SEM, EDX and UV-Visible spectral analysis. The wurtzite and cubic structure of ZnO/MgO nanocomposite has been confirmed by XRD and fluorescence studies. Above that, the SEM analysis assure about the flake like morphology of the nanocomposite which is responsible for the enhanced photocatalytic performance and crystalline nature of the prepared ZnO/MgO nanocomposite. The presence of zinc, magnesium and oxygen is approved by EDX analysis. The photocatalytic activity of the nanocomposite in the presence of visible light for the degradation of Quinalphos at neutral pH within forty minutes has been authorised by UV-Visible spectroscopy. The total organic carbon of the Quinalphos test solution has shown 90% reduction which confirmed the remarkable activity of the prepared composite. The prepared nanocomposite also exhibits a good recycling ability and this assures the quality of the catalyst. Hence the response of the prepared ZnO/MgO nano composite in sunlight provides an energetic and cost-effective technology for the treatment of waste water and other organic contaminants present in water within a short span of time.

Acknowledgement

The authors are thankful for Nesamony Memorial Christian College, Marthandam, India; Ayya Nadar Janaki Ammal College, Sivakasi, India; Vellore Institute of Technology, Chennai, India; and Karunya institute of technology and science, Coimbatore, India for furnishing necessary provision and support for this work.

References

- Gola D, Kriti A, Bhatt N, Bajpai M, Singh A, Arya A, Chauhan N, Srivatsava S K, Tyagi P K & Agarwal Y, *Curr Res Green Sustain Chem*, 4 (2021) Article 100132.
- Kamble R, Sabale S, Chikode P, Puri V & Mahajan S, *Indian J Chem*, 56A (2017) 479.
- Hemalatha D, Amala A, Rangasamy B, Nataraj B & Ramesh M, *Environ Toxicol*, 31 (2016) 1399.
- Sudheere M, Ravinder G, Ravi G, Venkataswamy P, Vaishnavi K, Chittibabu N & Vithal M, *Indian J Chem*, 59A (2020) 1092.
- Qi K & Yu J, *Interface Sci Technol*, 31 (2020) 265.
- Bhole D K, Puri R G, Meshram P D & Sirsam R S, *J Indian Chem Soc*, 97 (2020) 440.
- Samsudin E M, Gho S N, Wu T Y, Ling T T, Hamid S B A & Juan J C, *Sains Malays*, 44(7) (2015) 1011.
- Mathiarasu R R, Manikandan A, Panneerselvam K, George M, Raja K K, Almessiere M A, Slimani Y, Baykal A, Ansari A, Kamal T & Khan A, *J Mater Res Technol*, 15 (2021) 5936.
- Josephine S G A & Sivasamy A, *Indian J Chem*, 59A (2020) 1259.
- M Nirmala & A Anukaliani, *Mater Lett*, 65 (2011) 2645.
- Anandan S, Vinu A, Lovely K L P S, Gokulakrishnan N, Srinivasu P, Mori T, Murugesan V & Ariga K, *J Mol Catal A Chem*, 266 (2007) 149.
- Belver C, Bedia J, Gomez-Avilies A, Penas-Garzon M & Rodriguez J J, *Nanoscale in water purification*, (Elsevier, Amsterdam, Netherlands) (2019), pp.581.
- Ali A M, Muhammad A, Shafeeq A, Asghar H M, Hussain N & Sattar H, *J Pak Inst Chem Eng*, 40 (2012) 11.
- M F M Taib, D T Mustaffa, N H Hussin, M H Samat, M Z A Yahya, *Mater Res. Express*, 6, (2019) 1.
- Garg R, Gupta R, Sing N & Bansal A, *Chemosphere*, 286 (2022) Article 131837.
- Kaur P, Bansal P & Sud D, *J Korean Chem Soc*, 57 (2013) 382.
- Sharotri N, Sharma D & Sud D, *J Mater Res Technol*, 8 (2019) 3995.
- Das S & srivasatava V C, *Smart Sci*, 4 (2016) 190.
- Subha P P & Jayaraj M K, *J Exp Nanosci*, 10 (2015) 1106.
- A Rafiq, M Ikram, S Ali, F Niaz, M Khan, Q Khan & Maqbool M, *J Ind Eng Chem*, 97 (2021) 111.
- Dhanjal N I K, Kaur P, Sud D, Cameotra S S, *Water Environ Res*, 86 (2014) 457.
- Lin L, Han Y, Fuji M, Endo T, Wang X & Takahashi M, *J Ceram Soc Jpn*, 116 (2008) 198.
- Sutapa I W, Wahab A W, Taba P & Nafie N L, *Orient J Chem*, 34 (2018) 1016.
- Tang Y, Wee P, Lai Y, Wang X, Gong D, Kanhere P D, Lim T T, Dong Z & Chen Z, *J Phys Chem C*, 116 (2012) 2772.
- Kiwaan H A, Atwee T M, Azab E A & El-Bindary A A, *J Mol Struct*, 1200 (2020) Article 127115.
- Alshabanat M N & Al-Anazy M M, *J Chem*, (2018) Article ID 9651850.
- Lekota M W, Dimple K M & Nomngongo P N, *J Anal Sci Technol*, 10 (2019) 1.
- Chawla S, Jayanthi K, Chander H, Halder S K & Kar M, *J Alloys Compd*, 459 (2008) 457.
- Anaam S A A, Saim H, Sahdan M Z & Al-Gheethi A, *Int J Nanoelectron Mater*, 12 (2019) 495.
- Byrappa K, Subramani A K, Ananda S, Rai K M L, Dinesh R & Yoshimura M, *Bull Mater Sci*, 29 (2006) 433.
- Kus M, Ribbens S, Meynen V & Cool P, *Catalyst*, 3 (2013) 74.
- Zeng Q, Liu Y, Shen L, Lin H, Yu W, Xu Y, Li R & Huang L, *J Colloid Interface Sci*, 582 (2021) 291.